

# WATER VAPOR EMISSION REVEALS A HIGHLY OBSCURED, STAR FORMING NUCLEAR REGION IN THE QSO HOST GALAXY APM08279+5255 AT $Z=3.9$

PAUL P. VAN DER WERF<sup>1,2</sup>, A. BERCIANO ALBA<sup>3,1</sup>, M. SPAANS<sup>4</sup>, A.F. LOENEN<sup>1</sup>, R. MEIJERINK<sup>1</sup>, D.A. RIECHERS<sup>5</sup>,  
P. COX<sup>6</sup>, F. WALTER<sup>7</sup>, A. WEISS<sup>8</sup>

*in preparation for the Astrophysical Journal Letters*

## ABSTRACT

We present the detection of four rotational emission lines of water vapor, from energy levels  $E_u/k = 101 - 454$  K, in the gravitationally lensed  $z = 3.9$  QSO host galaxy APM08279+5255. While the lowest H<sub>2</sub>O lines are collisionally excited in clumps of warm, dense gas, we find that the excitation of the higher lines is dominated by the intense local infrared radiation field, giving rise to line ratios that strongly deviate from those in prominent Galactic star forming regions. Our excitation model requires the emitting gas to be located in an extended region of high  $100 \mu\text{m}$  opacity. Locally, such extended infrared-opaque regions are found only in the nuclei of ultraluminous infrared galaxies. We propose a model where the infrared-opaque disk, which is penetrated by the X-ray radiation field of the QSO nucleus, contains clumps of massive star formation where the H<sub>2</sub>O emission originates. Analysis of local conditions indicates Eddington-limited star formation in these clumps.

*Subject headings:* galaxies: ISM — galaxies: nuclei — quasars: individual (APM08279+5255)

## 1. INTRODUCTION

Water is expected to be one of the most abundant molecules in molecular clouds in galaxies. In cold molecular clouds water is in the form of icy mantles on dust grains, with total H<sub>2</sub>O abundances up to  $10^{-4}$  with respect to hydrogen nuclei (Tielens et al. 1991), thus containing up to 30% of the available oxygen atoms. In warm molecular clouds, such as in star forming galaxies or galaxies with a luminous active galactic nucleus, water can be released from the dust grains, or form directly in the gas phase, and is believed to play a key role as cooling agent of the warm, dense gas clouds (Neufeld & Kaufman 1993; Neufeld et al. 1995).

Due the wet Earth atmosphere, bulk gas-phase water can only be detected from space, or from distant objects where the cosmological redshift moves the H<sub>2</sub>O lines into transparent atmospheric windows. Despite several previous searches for rotational emission lines of H<sub>2</sub>O from high- $z$  objects (Wagg et al. 2006; Riechers et al. 2006, 2009b), the first detection of H<sub>2</sub>O emission from a high redshift objects has been achieved only recently, in a gravitationally lensed galaxy at  $z = 2.3$  (Omont et al. 2011). However, since only one line was detected, it was not possible to address the molecular excitation mecha-

nism. Furthermore, since the line was optically thick, no water abundance could be derived.

The Herschel Space Observatory has recently enabled the first detections of H<sub>2</sub>O emission lines from two nearby galaxies, with very different results between the two objects (Van der Werf et al. 2010; González-Alfonso et al. 2010; Weiß et al. 2010). Spectra of the lowest H<sub>2</sub>O transitions in the nearby starburst galaxy M82 revealed faint lines with complex spectral shapes, with one of the lines (the  $1_{1,1} - 0_{0,0}$  para-H<sub>2</sub>O ground-state line) appearing in absorption (Weiß et al. 2010). No H<sub>2</sub>O emission from higher rotational levels was found (Panuzzo et al. 2010). In marked contrast, the nearby Ultraluminous Infrared Galaxy (ULIRG) and QSO Mrk 231 revealed a rich spectrum of H<sub>2</sub>O lines from upper level energies  $E_u$  up to  $E_u/k = 640$  K (where  $k$  is the Boltzmann constant), whereas the lower lines connecting to the ground state remained undetected (Van der Werf et al. 2010).

In order to search for H<sub>2</sub>O in a high- $z$  galaxy in a systematic way, we undertook a search for four lines of H<sub>2</sub>O, with a range of upper level energies, in the gas-rich gravitationally lensed  $z = 3.9$  QSO host galaxy APM08279 + 5255 (Irwin et al. 1998; Lewis et al. 1998). With CO lines detected from rotational levels up to  $J = 11$  (Weiß et al. 2007; Riechers et al. 2009b) and HCN, HNC and HCO<sup>+</sup> lines from levels up to  $J = 6$  (Riechers et al. 2010), its molecular medium has been characterized better than any other high- $z$  galaxy, and indeed better than most galaxies at any redshift. Analysis of the CO rotational ladder revealed unusually high excitation (Weiß et al. 2007). However, a previous search for the ortho ground-state  $1_{1,0} - 1_{0,1}$  H<sub>2</sub>O line was unsuccessful (Wagg et al. 2006). We therefore targeted lines of higher excitation, with upper level energies  $E_u/k$  from 101 to 454 K.

## 2. OBSERVATIONS AND RESULTS

We used the IRAM Plateau de Bure Interferometer (Guilloteau et al. 1992) between December 2010 and March 2011 to observe the four H<sub>2</sub>O lines listed in Table 1

<sup>1</sup> Leiden Observatory, Leiden University, P.O. Box 9513, NL-2300 RA Leiden, The Netherlands

<sup>2</sup> SUPA, Institute of Astronomy, University of Edinburgh, Royal Observatory, Blackford Hill, Edinburgh EH9 3HJ, United Kingdom

<sup>3</sup> ASTRON, P.O. Box 2, NL-2990 AA Dwingeloo, The Netherlands

<sup>4</sup> Kapteyn Astronomical Institute, University of Groningen, P.O. Box 800, NL-9700 AV Groningen, The Netherlands

<sup>5</sup> Astronomy Department, California Institute of Technology, MC 249-17, 1200 East California Boulevard, Pasadena, CA 91125, USA

<sup>6</sup> IRAM, 300 Rue de la Piscine, 38406 St. Martin d'Heres, Grenoble, France

<sup>7</sup> Max-Planck-Institut für Astronomie, Königstuhl 17, Heidelberg, D-69117, Germany

<sup>8</sup> Max-Planck-Institut für Radioastronomie, Auf dem Hügel 16, Bonn, D-53121, Germany

TABLE 1  
PARAMETERS OF H<sub>2</sub>O LINES DETECTED IN APM08279+5255

Line	$\nu_0^a$ [GHz]	$E_u/k^b$ [K]	$S_{\text{line}}^c$ [Jy km s <sup>-1</sup> ]	$S_{\text{model}}^d$ [Jy km s <sup>-1</sup> ]
1 <sub>1,0</sub> – 1 <sub>0,1</sub>	556.936	61	<0.7	0.16
2 <sub>0,2</sub> – 1 <sub>1,1</sub>	987.926	101	5.3 ± 0.5	5.9
2 <sub>1,1</sub> – 2 <sub>0,2</sub>	752.033	137	4.5 ± 0.3	4.4
3 <sub>2,1</sub> – 3 <sub>1,2</sub>	1162.911	305	9.3 ± 1.4	9.2
4 <sub>2,2</sub> – 4 <sub>1,3</sub>	1207.638	454	2.5 ± 0.3	2.7

<sup>a</sup>Rest frequency of the line

<sup>b</sup>Upper level energy of the transition

<sup>c</sup>Observed integrated line flux; all measurements are from this work except the 1<sub>1,0</sub> – 1<sub>0,1</sub> upper limit (Wagg et al. 2006)

<sup>d</sup>Modeled integrated line flux

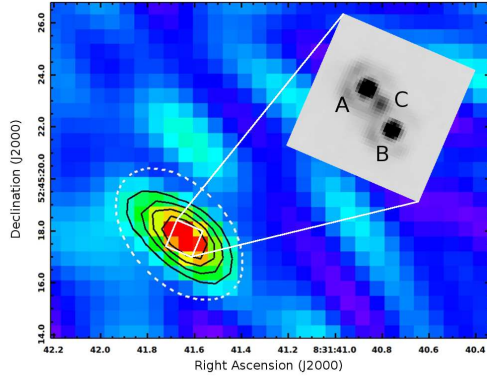


FIG. 1.— H<sub>2</sub>O emission from APM08279+5255. The contoured pseudocolor map shows the distribution of the velocity-integrated continuum-subtracted H<sub>2</sub>O 2<sub>1,1</sub> – 2<sub>0,2</sub> line flux, with contour levels of 3, 5, 7 and 9 $\sigma$ , where  $\sigma = 0.5$  Jy km s<sup>-1</sup> beam<sup>-1</sup>. The dashed white ellipse indicates the synthesized beam of 3''0 × 1''9, at a position angle of 47°. The inset presents the NICMOS F110W image (Ibata et al. 1999) and shows that the gravitationally lensed images (the brightest of which are 0''378 apart) are fully covered by the synthesized beam.

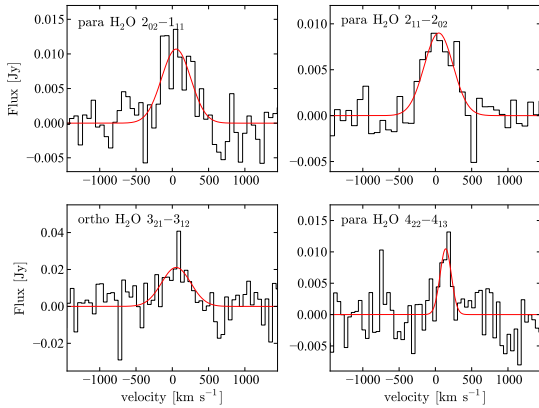


FIG. 2.— Spectra of H<sub>2</sub>O emission lines from APM08279+5255, after subtraction of the continuum. The horizontal axis shows velocity relative to redshift  $z = 3.911$ . The red curves indicate Gaussian fits to each spectrum.

in APM08279+5255. The observations were carried out in D and C-configuration, ensuring that the gravitationally lensed images are all fully contained within one synthesized beam, at all observing frequencies. All four lines were detected and an image of the flux distribution of the 2<sub>1,1</sub> – 2<sub>0,2</sub> line is shown in Fig. 1. Spectra of the four H<sub>2</sub>O

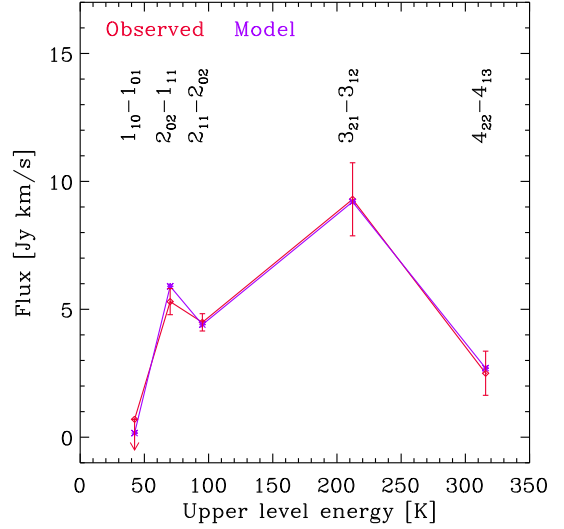


FIG. 3.— Flux in H<sub>2</sub>O emission lines from APM08279+5255 as a function of upper level energy  $E_u$ . Red symbols and error bars indicate the observed line fluxes and the previously published upper limit on 1<sub>1,0</sub> – 1<sub>0,1</sub> (indicated by a downward arrow). Purple crosses indicate values produced by our model described in the text.

lines are shown in Fig. 2 and parameters of the detected lines are presented in Table 1. As expected from the angular resolution of our observations and the angular size of the CO emission (0''4 Riechers et al. 2009b), all our detections show spatially unresolved emission. The most sensitive detection is that of the 2<sub>1,1</sub> – 2<sub>0,2</sub> line, which displays a symmetric line profile with the full width at half maximum (FWHM) of 470 km s<sup>-1</sup>, excellently matching the widths of the CO lines (Weiß et al. 2007). The 3<sub>2,1</sub> – 3<sub>1,2</sub> and 2<sub>0,2</sub> – 1<sub>1,1</sub> lines display similar widths, but the 4<sub>2,2</sub> – 4<sub>1,3</sub> line is distinctly narrower with a FWHM of only 200 km s<sup>-1</sup>. Recently, a low spectral resolution 1 mm spectrum of APM081279+5255 obtained with Z-Spec has been released by Bradford et al. (2011). This spectrum confirms our detection of prominent 3<sub>2,1</sub> – 3<sub>1,2</sub> and fainter 4<sub>2,2</sub> – 4<sub>1,3</sub> emission, but also reveals a number of discrepancies. First, our measured flux of the 3<sub>2,1</sub> – 3<sub>1,2</sub> line is a factor 1.7 fainter than the values reported by Bradford et al. (2011), and this discrepancy is similar to that between the CO line fluxes measured from Z-Spec and from the IRAM 30 m telescope (Weiß et al. 2007). A larger discrepancy exists for the 4<sub>2,2</sub> – 4<sub>1,3</sub> line, where our flux is factor of 5 lower than the Z-Spec value. Finally, the Z-Spec spectrum does not detect the 2<sub>0,2</sub> – 1<sub>1,1</sub> line, which is well detected in our data.

### 3. FAR-IR PUMPED H<sub>2</sub>O EMISSION

The distribution of the detected line flux as a function of the energy of the upper level of the transition is shown in Fig. 3. The flux distribution peaks at the 3<sub>2,1</sub> – 3<sub>1,2</sub> line, implying that for purely collisional excitation the gas temperature must be of the order of at least 200 K. Critical densities are approximately 10<sup>8</sup> cm<sup>-3</sup> for the lowest lines (2<sub>0,2</sub> – 1<sub>1,1</sub> and 2<sub>1,1</sub> – 2<sub>0,2</sub>) and higher than 10<sup>8</sup> cm<sup>-3</sup> for the higher lines. Therefore, any purely collisionally excited model that can account for the observed 3<sub>2,1</sub> – 3<sub>1,2</sub> and 4<sub>2,2</sub> – 4<sub>1,3</sub> fluxes would produce strong emission in the lower lines, including the 1<sub>1,0</sub> – 1<sub>0,1</sub>

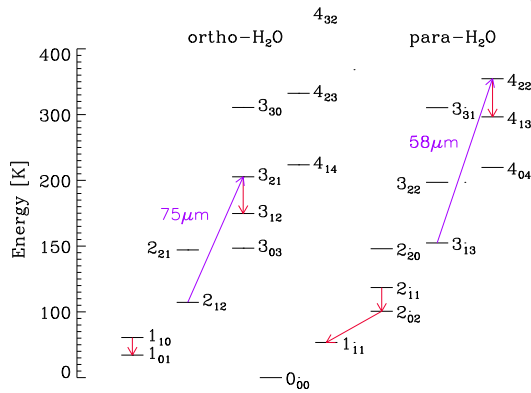


FIG. 4.— Partial H<sub>2</sub>O energy level diagram. The ortho and para-H<sub>2</sub>O rotational ladders are indicated, and the transitions detected here, as well as the upper limit on the 1<sub>1,0</sub> – 1<sub>0,1</sub> ortho-H<sub>2</sub>O ground state transition are indicated by red arrows. Purple arrows indicate the radiative pumping transitions at 58 and 75  $\mu$ m that account for the efficient population of the 4<sub>2,2</sub> and 3<sub>2,1</sub> levels.

level, for which a sensitive upper limit exists (Wagg et al. 2006). We therefore rule out purely collisional excitation and consider in addition radiative excitation by an intense far-infrared (far-IR) radiation field from warm dust, with a temperature  $T_d = 220$  K, as derived from the continuum spectral energy distribution (Weiß et al. 2007; Riechers et al. 2009b).

We model these coupled processes using a radiative transfer code (Poelman & Spaans 2005, 2006) which computes the statistical equilibrium populations of all relevant H<sub>2</sub>O levels in the ground and first vibrationally excited state. Line radiation is transferred in a non-local and three-dimensional manner through a multi-zone escape probability calculation. The model consists of dense clumps within a spherical region with a radius of 100 pc. Due to the high critical densities of the H<sub>2</sub>O lines, only the clumps contribute to the H<sub>2</sub>O emission, and we have run a model grid with clump densities  $n_H = 10^5 - 10^7$  cm<sup>-3</sup>, gas temperatures  $T_g = 50 - 200$  K, and H<sub>2</sub>O column densities  $10^{16} - 10^{18}$  cm<sup>-2</sup>. The H<sub>2</sub>O ortho-to-para ratio was obtained from thermal equilibrium (Poelman & Spaans 2005) and found to be very close to the statistical equilibrium value of 3. We adopt a gas-to-dust mass ratio of 100, a radial grid resolution of 200 points and a local turbulent velocity dispersion of 4 km s<sup>-1</sup>, with a total velocity difference (gradient times length) across the model region of 140 km s<sup>-1</sup>. The latter yields line widths consistent with the observed FWHM of 200 km s<sup>-1</sup> of the marginally optically thin 4<sub>2,2</sub> – 4<sub>1,3</sub> line.

In our best fit model, the clumps have a density of hydrogen nuclei  $n_H = 2 \times 10^6$  cm<sup>-3</sup>, a gas temperature  $T_g = 120$  K, and the average density of hydrogen nuclei over the 100 pc radius model region is  $\langle n_H \rangle = 3000$  cm<sup>-3</sup>, yielding a 100  $\mu$ m continuum optical depth  $\tau_{100} \approx 0.7$ . The line fluxes predicted by this model are listed in Table 1 and shown in Fig. 3. The lowest levels (up to 2<sub>1,1</sub> – 2<sub>0,2</sub>) are excited mostly by collisions. The clump density and temperature derived in our model are determined by these lines, and the required density is somewhat higher than that derived for the CO lines (Weiß et al. 2007), which is not surprising given the higher critical densities of the H<sub>2</sub>O lines. In contrast, the 4<sub>2,2</sub> and 3<sub>2,1</sub> levels are populated exclusively

by the absorption of far-IR photons. As shown in Fig. 4, the pumping occurs at 58 and 75  $\mu$ m rest frame wavelengths. The intensity of the radiatively excited lines provides a measure of the intensity of the local far-IR radiation field and therefore of the optical depth in the spectral region of the pumping wavelengths, and this determines the 100  $\mu$ m optical depth in our model. The relative strengths of the 4<sub>2,2</sub> – 4<sub>1,3</sub> and 3<sub>2,1</sub> – 3<sub>1,2</sub> lines in principle provides a measurement of the colour temperature of the far-IR radiation field, but for  $T_d > 100$  K the pumping wavelengths are on the Rayleigh-Jeans tail of the warm dust continuum, making the line ratio insensitive to the dust temperature. Since only collisionally excited lines contribute to the cooling (i.e., removal of kinetic energy) of warm molecular gas, we find that cooling by the H<sub>2</sub>O lines is unimportant compared to the cooling by CO lines, in contrast to the conclusion by Bradford et al. (2011) and to earlier theoretical suggestions (Neufeld & Kaufman 1993; Neufeld et al. 1995). We note that radiative excitation has also been suggested to drive the intensity of HCN lines in APM 08279+5255 (García-Burillo et al. 2006; Weiß et al. 2007).

In our best fit model, the 4<sub>2,2</sub> – 4<sub>1,3</sub> line is almost optically thin (optical depth approximately unity) and allows a determination of the total column density of warm ( $T_g > 100$  K) water vapor. We find a (beam-averaged) warm H<sub>2</sub>O column density of  $1.2 \times 10^{17}$  cm<sup>-2</sup>, i.e., a warm H<sub>2</sub>O/H<sub>2</sub> abundance of approximately  $3 \times 10^{-7}$ , consistent with ultraviolet or X-ray irradiated chemical models (Meijerink & Spaans 2005). Since the other lines have line centre optical depths from 30 to 300 in our model, these lines are expected to be significantly broader in velocity than the 4<sub>2,2</sub> – 4<sub>1,3</sub> line, and this is in fact observed (Fig. 2).

#### 4. IMPLICATIONS FOR THE NUCLEAR REGION OF APM 08279+5255

The H<sub>2</sub>O line ratios observed in APM 08279+5255 are unlike any object observed in the Milky Way. Water lines from ultraviolet irradiated gas (photon-dominated regions or PDRs) in prominent Galactic star forming regions show thermal level populations (White et al. 2010; Habart et al. 2010), dominated by low-lying lines, showing only faint emission, at levels much lower than CO lines in the same frequency range. The best case in point is the prominent Orion Bar PDR where only a few low lying H<sub>2</sub>O lines are detected (Habart et al. 2010), and the 2<sub>1,1</sub> – 2<sub>0,2</sub>/1<sub>1,0</sub> – 1<sub>0,1</sub> luminosity ratio is 0.6; in contrast, in APM 08279+5255, this ratio is  $> 6.4$ . Furthermore, in APM 08279+5255, the H<sub>2</sub>O lines have luminosities comparable to nearby CO lines, while they are two orders of magnitude fainter in the Orion Bar (e.g., the H<sub>2</sub>O 2<sub>1,1</sub> – 2<sub>0,2</sub> / CO(6–5) line luminosity ratio is 0.6 in APM 08279+5255, while it is 0.026 in the Orion Bar). The only object with properties comparable to APM 08279+5255 is the nearby ULIRG/QSO Mrk 231 (Van der Werf et al. 2010), where high H<sub>2</sub>O lines were also found to be radiatively excited (González-Alfonso et al. 2010), although the effect is even stronger in APM 08279+5255, which has a 3<sub>2,1</sub> – 3<sub>1,2</sub>/2<sub>0,2</sub> – 1<sub>1,1</sub> luminosity ratio of 1.8, compared to 0.9 in Mrk 231.

The fact that in the presence of an intense far-IR radiation field the most luminous H<sub>2</sub>O emission is radiatively

excited follows directly from the large Einstein  $A$ -values of the  $\text{H}_2\text{O}$  rotational lines, which result in high critical densities as well as a strong coupling to the local far-IR radiation field. A key result of our analysis is therefore the presence of a sufficiently intense local far-IR radiation field, which requires the emitting clumps to be located in a very obscured environment, with  $\tau_{100} \approx 0.7$ . The high dust temperature  $T_d = 220$  K favors a PDR over an X-ray dominated region (XDR), since in contrast to PDRs, high dust temperatures are not easily achieved in XDRs (Meijerink & Spaans 2005). The essential difference with the Orion Bar PDR (aside from less important differences in temperature and density) is the fact that the latter is not optically thick at  $100 \mu\text{m}$ , while in APM08279+5255  $\tau_{100} \approx 0.7$  over the entire region sampled, i.e., several hundred pc. The observationally derived size of this region depends on the details of the lensing model (Weiß et al. 2007; Riechers et al. 2009b), and the most recent analysis, which accurately reproduces the positions and luminosities of the gravitationally lensed images of the QSO nucleus, gives an intrinsic CO(1–0) source radius of up to 500 pc with an extended continuum of about 1 kpc size, at an inclination of less than  $30^\circ$  from face-on (Riechers et al. 2009b).

The CO rotation line ladder of APM08279+5255 shows even higher excitation than that of Mrk231 and therefore most likely reveals the presence of an XDR (Weiß et al. 2007; Van der Werf et al. 2010). Since high  $\text{H}_2\text{O}$  abundances can be generated in both PDRs and XDRs Meijerink & Spaans (2005), our data do not distinguish directly between these models, but as noted above, the high dust temperature of  $\sim 200$  K over a  $\sim 500$  pc radius region is more easily achieved in PDRs, generated by widespread star formation in clumps of dense gas throughout the circumnuclear gas disk. Regions of several 100 pc radius, with high  $100 \mu\text{m}$  optical depths, are locally found only in the central regions of ULIRGs (Solomon et al. 1997). The fact that in this study we find such a region in a QSO, provides support for the scenario where ULIRGs form the birthplaces of QSOs (Sanders et al. 1988). The presence of widespread massive star formation in the infrared-opaque nuclear medium shows that in this object the buildup of the supermassive black hole and the nuclear stellar population are proceeding simultaneously.

What can we say about local conditions in this dense and opaque star forming medium? The circumnuclear star formation in APM08279+5255 takes places in the presence of a strong and penetrative X-ray radiation field. As shown by Hocuk & Spaans (2010), in this situation fragmentation is inhibited and a top-heavy stellar Initial Mass Function is expected to result. It is possible that this effect accounts for the extraordinary far-IR luminosity  $L_{\text{FIR}} = 5 \times 10^{13} L_\odot$  (corrected for a factor  $\mu = 4$  gravitational amplification, Riechers et al. 2009a) of APM08279+5255. We note also that in the star forming clumps in our model, both turbulent pressure  $P_{\text{turb}} \sim \rho \sigma_v^2/3$  (where  $\rho$  is the mass density of the gas clump and  $\sigma_v$  = its turbulent velocity dispersion) and radiation pressure  $P_{\text{rad}} \sim \tau_{100} \sigma T_d^4/c$  (where  $\sigma$  is the Stefan-Boltzmann constant and  $c$  the speed of light) exceed the thermal pressure  $P_{\text{th}} \sim n_{\text{H}_2} k T_g$  by a large factor. Inserting numbers from our best-fit model, we find that  $P_{\text{th}} \sim 2 \times 10^{-8} \text{ erg cm}^{-3}$ , while  $P_{\text{turb}} \sim P_{\text{rad}} \sim 2.2 \times 10^{-7} \text{ erg cm}^{-3}$ . Given the importance of radiation pressure, the star formation process is close to Eddington-limited, as proposed by Thompson et al. (2005) for starburst disks feeding a central supermassive black hole.

Our study demonstrates how radiatively exited  $\text{H}_2\text{O}$  lines can be used to reveal the presence of extended infrared-opaque regions in galactic nuclei (even without spatially resolving these regions). Furthermore, we can derive local conditions in the infrared-opaque nuclear gas disk, which in the present case indicates close to Eddington-limited star formation. While for local galaxies observations from space will remain necessary to observe the  $\text{H}_2\text{O}$  lines, the Atacama Large Millimeter Array will make this diagnostic readily available in galaxies with sufficient redshift, without the aid of gravitational lensing.

This work is based on observations carried out with the IRAM Plateau de Bure Interferometer. IRAM is supported by INSU/CNRS (France), MPG (Germany) and IGN (Spain). DR acknowledges support from NASA through a Spitzer grant. We thank Melanie Krips for expert assistance with the IRAM data reduction.

Facilities: IRAM Plateau de Bure Interferometer

## REFERENCES

- Bradford, C. M., Bolatto, A. D., Maloney, P. R., Aguirre, J. E., Bock, J. J., Glenn, J., Kamenetzky, J., Lupu, R., Matsuhara, H., Murphy, E. J., Naylor, B. J., Nguyen, H. T., Scott, K., & Zmuidzinas, J. 2011, ArXiv e-prints
- García-Burillo, S., Graciá-Carpio, J., Guélin, M., Neri, R., Cox, P., Planesas, P., Solomon, P. M., Tacconi, L. J., & Vanden Bout, P. A. 2006, *ApJ*, 645, L17
- González-Alfonso, E., Fischer, J., Isaak, K., Rykala, A., Savini, G., Spaans, M., van der Werf, P., Meijerink, R., Israel, F. P., Loenen, A. F., Vlahakis, C., Smith, H. A., Charmandaris, V., Aalto, S., Henkel, C., Weiß, A., Walter, F., Greve, T. R., Martín-Pintado, J., Naylor, D. A., Spinoglio, L., Veilleux, S., Harris, A. I., Armus, L., Lord, S., Mazzarella, J., Xilouris, E. M., Sanders, D. B., Dasyra, K. M., Wiedner, M. C., Kramer, C., Papadopoulos, P. P., Stacey, G. J., Evans, A. S., & Gao, Y. 2010, *A&A*, 518, L43+
- Guilloteau, S., Delannoy, J., Downes, D., Greve, A., Guelin, M., Lucas, R., Morris, D., Radford, S. J. E., Wink, J., Cernicharo, J., Forveille, T., García-Burillo, S., Neri, R., Blondel, J., Perrigourad, A., Plathner, D., & Torres, M. 1992, *A&A*, 262, 624
- Habart, E., Dartois, E., Abergel, A., Baluteau, J., Naylor, D., Polehampton, E., Joblin, C., Ade, P., Anderson, L. D., André, P., Arab, H., Bernard, J., Blagrove, K., Bontemps, S., Boulanger, F., Cohen, M., Compiegne, M., Cox, P., Davis, G., Emery, R., Fulton, T., Gry, C., Huang, M., Jones, S. C., Kirk, J., Lagache, G., Lim, T., Madden, S., Makiwa, G., Martin, P., Miville-Deschênes, M., Molinari, S., Moseley, H., Motte, F., Okumura, K., Pinheiro Gonçalves, D., Rodon, J., Russeil, D., Saraceno, P., Sidher, S., Spencer, L., Swinyard, B., Ward-Thompson, D., White, G. J., & Zavagno, A. 2010, *A&A*, 518, L116+
- Hocuk, S. & Spaans, M. 2010, *A&A*, 522, A24+
- Ibata, R. A., Lewis, G. F., Irwin, M. J., Lehár, J., & Totten, E. J. 1999, *AJ*, 118, 1922

- Irwin, M. J., Ibata, R. A., Lewis, G. F., & Totten, E. J. 1998, *ApJ*, 505, 529
- Lewis, G. F., Chapman, S. C., Ibata, R. A., Irwin, M. J., & Totten, E. J. 1998, *ApJ*, 505, L1+
- Meijerink, R. & Spaans, M. 2005, *A&A*, 436, 397
- Neufeld, D. A. & Kaufman, M. J. 1993, *ApJ*, 418, 263
- Neufeld, D. A., Lepp, S., & Melnick, G. J. 1995, *ApJS*, 100, 132
- Omont, A., Neri, R., Cox, P., Lupu, R., Guélin, M., van der Werf, P., Weiß, A., Ivison, R., Negrello, M., Leeuw, L., Lehnert, M., Smail, I., Verma, A., Baker, A. J., Beelen, A., Aguirre, J. E., Baes, M., Bertoldi, F., Clements, D. L., Cooray, A., Coppin, K., Dannerbauer, H., de Zotti, G., Dye, S., Fiolet, N., Frayer, D., Gavazzi, R., Hughes, D., Jarvis, M., Krips, M., Michałowski, M. J., Murphy, E. J., Riechers, D., Serjeant, S., Swinbank, A. M., Temi, P., Vaccari, M., Vieira, J. D., Auld, R., Buttiglione, B., Cava, A., Dariush, A., Dunne, L., Eales, S. A., Fritz, J., Gomez, H., Ibar, E., Maddox, S., Pascale, E., Pohlen, M., Rigby, E., Smith, D. J. B., Bock, J., Bradford, C. M., Glenn, J., Scott, K. S., & Zmuidzinas, J. 2011, *A&A*, 530, L3+
- Panuzzo, P., Rangwala, N., Rykala, A., Isaak, K. G., Glenn, J., Wilson, C. D., Auld, R., Baes, M., Barlow, M. J., Bendo, G. J., Bock, J. J., Boselli, A., Bradford, M., Buat, V., Castro-Rodríguez, N., Chanial, P., Charlot, S., Ciesla, L., Clements, D. L., Cooray, A., Cormier, D., Cortese, L., Davies, J. I., Dwek, E., Eales, S. A., Elbaz, D., Fulton, T., Galametz, M., Galliano, F., Gear, W. K., Gomez, H. L., Griffin, M., Hony, S., Levenson, L. R., Lu, N., Madden, S., O'Halloran, B., Okumura, K., Oliver, S., Page, M. J., Papageorgiou, A., Parkin, T. J., Pérez-Fournon, I., Pohlen, M., Polehampton, E. T., Rigby, E. E., Roussel, H., Sacchi, N., Sauvage, M., Schulz, B., Schirm, M. R. P., Smith, M. W. L., Spinoglio, L., Stevens, J. A., Srinivasan, S., Symeonidis, M., Swinyard, B., Trichas, M., Vaccari, M., Vigroux, L., Wozniak, H., Wright, G. S., & Zeilinger, W. W. 2010, *A&A*, 518, L37+
- Poelman, D. R. & Spaans, M. 2005, *A&A*, 440, 559
- . 2006, *A&A*, 453, 615
- Riechers, D. A., Walter, F., Bertoldi, F., Carilli, C. L., Aravena, M., Neri, R., Cox, P., Weiß, A., & Menten, K. M. 2009a, *ApJ*, 703, 1338
- Riechers, D. A., Walter, F., Carilli, C. L., & Lewis, G. F. 2009b, *ApJ*, 690, 463
- Riechers, D. A., Weiss, A., Walter, F., Carilli, C. L., & Knudsen, K. K. 2006, *ApJ*, 649, 635
- Riechers, D. A., Weiß, A., Walter, F., & Wagg, J. 2010, *ApJ*, 725, 1032
- Sanders, D. B., Soifer, B. T., Elias, J. H., Madore, B. F., Matthews, K., Neugebauer, G., & Scoville, N. Z. 1988, *ApJ*, 325, 74
- Solomon, P. M., Downes, D., Radford, S. J. E., & Barrett, J. W. 1997, *ApJ*, 478, 144
- Thompson, T. A., Quataert, E., & Murray, N. 2005, *ApJ*, 630, 167
- Tielens, A. G. G. M., Tokunaga, A. T., Geballe, T. R., & Baas, F. 1991, *ApJ*, 381, 181
- Van der Werf, P. P., Isaak, K. G., Meijerink, R., Spaans, M., Rykala, A., Fulton, T., Loenen, A. F., Walter, F., Weiß, A., Armus, L., Fischer, J., Israel, F. P., Harris, A. I., Veilleux, S., Henkel, C., Savini, G., Lord, S., Smith, H. A., González-Alfonso, E., Naylor, D., Aalto, S., Charmandaris, V., Dasyra, K. M., Evans, A., Gao, Y., Greve, T. R., Güsten, R., Kramer, C., Martín-Pintado, J., Mazzarella, J., Papadopoulos, P. P., Sanders, D. B., Spinoglio, L., Stacey, G., Vlahakis, C., Wiedner, M. C., & Xilouris, E. M. 2010, *A&A*, 518, L42+
- Wagg, J., Wilner, D. J., Neri, R., Downes, D., & Wiklind, T. 2006, *ApJ*, 651, 46
- Weiß, A., Downes, D., Neri, R., Walter, F., Henkel, C., Wilner, D. J., Wagg, J., & Wiklind, T. 2007, *A&A*, 467, 955
- Weiß, A., Requena-Torres, M. A., Güsten, R., García-Burillo, S., Harris, A. I., Israel, F. P., Klein, T., Kramer, C., Lord, S., Martín-Pintado, J., Röllig, M., Stutzki, J., Szczerba, R., van der Werf, P. P., Philipp-May, S., Yorke, H., Akyilmaz, M., Gal, C., Higgins, R., Marston, A., Roberts, J., Schlöder, F., Schultz, M., Teyssier, D., Whyborn, N., & Wunsch, H. J. 2010, *A&A*, 521, L1+
- White, G. J., Abergel, A., Spencer, L., Schneider, N., Naylor, D. A., Anderson, L. D., Joblin, C., Ade, P., André, P., Arab, H., Baluteau, J.-P., Bernard, J.-P., Blagrove, K., Bontemps, S., Boulanger, F., Cohen, M., Compiègne, M., Cox, P., Dartois, E., Davis, G., Emery, R., Fulton, T., Gom, B., Griffin, M., Gry, C., Habart, E., Huang, M., Jones, S., Kirk, J. M., Lagache, G., Leeks, S., Lim, T., Madden, S., Makiwa, G., Martin, P., Miville-Deschênes, M.-A., Molinari, S., Moseley, H., Motte, F., Okumura, K., Pinheiro Gonçalves, D., Polehampton, E., Rodet, T., Rodón, J. A., Russeil, D., Saraceno, P., Sidher, S., Swinyard, B. M., Ward-Thompson, D., & Zavagno, A. 2010, *A&A*, 518, L114+